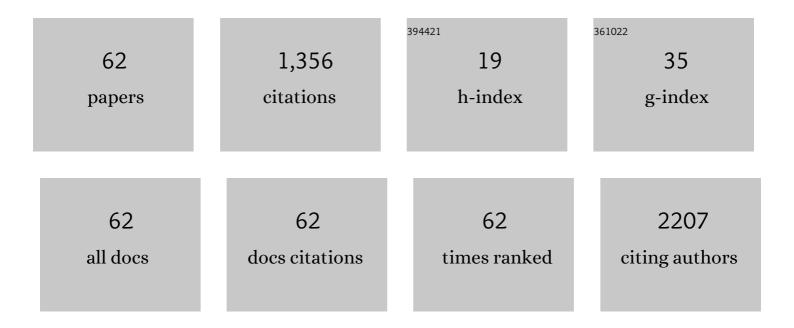
Francesco Carla

List of Publications by Year in descending order

Source: https://exaly.com/author-pdf/1636238/publications.pdf Version: 2024-02-01



#	Article	IF	CITATIONS
1	Structure of the Surface Region of Stainless Steel: Bulk and Thin Films. Physica Status Solidi (B): Basic Research, 2022, 259, .	1.5	5
2	Templated electrodeposition as a scalable and surfactant-free approach to the synthesis of Au nanoparticles with tunable aspect ratios. Nanoscale Advances, 2022, 4, 2452-2467.	4.6	5
3	Patterning enhanced tetragonality in <mml:math xmlns:mml="http://www.w3.org/1998/Math/MathML"><mml:mrow><mml:mi>Bi</mml:mi><mml:mi>Femathvariant="normal">O</mml:mi><mml:mn>3</mml:mn></mml:mrow> thin films with effective negative pressure by helium implantation. Physical Review Materials. 2021. 5.</mml:math 	i> <mml:n 2.4</mml:n 	nsub> <mml:r< td=""></mml:r<>
4	Quantitative powder diffraction using a (2â€+â€3) surface diffractometer and an area detector. Journal of Applied Crystallography, 2021, 54, 1140-1152.	4.5	6
5	Studying the onset of galvanic steel corrosion in situ using thin films: film preparation, characterization and application to pitting. Journal of Physics Condensed Matter, 2021, 33, 125001.	1.8	2
6	Organothiol Monolayer Formation Directly on Muscovite Mica. Angewandte Chemie, 2020, 132, 2343-2347.	2.0	1
7	Organothiol Monolayer Formation Directly on Muscovite Mica. Angewandte Chemie - International Edition, 2020, 59, 2323-2327.	13.8	4
8	Biogenic supported lipid bilayers as a tool to investigate nano-bio interfaces. Journal of Colloid and Interface Science, 2020, 570, 340-349.	9.4	24
9	Shedding light on membrane-templated clustering of gold nanoparticles. Journal of Colloid and Interface Science, 2020, 573, 204-214.	9.4	27
10	Redefining passivity breakdown of super duplex stainless steel by electrochemical operando synchrotron near surface X-ray analyses. Npj Materials Degradation, 2019, 3, .	5.8	36
11	Potential-Induced Pitting Corrosion of an IrO ₂ (110)-RuO ₂ (110)/Ru(0001) Model Electrode under Oxygen Evolution Reaction Conditions. ACS Catalysis, 2019, 9, 6530-6539.	11.2	43
12	A novel 3D printed radial collimator for x-ray diffraction. Review of Scientific Instruments, 2019, 90, 035102.	1.3	9
13	Influence of Surface Strain on Passive Film Formation of Duplex Stainless Steel and Its Degradation in Corrosive Environment. Journal of the Electrochemical Society, 2019, 166, C3071-C3080.	2.9	17
14	In Situ Studies of the Electrochemical Reduction of a Supported Ultrathin Single-Crystalline RuO ₂ (110) Layer in an Acidic Environment. Journal of Physical Chemistry C, 2019, 123, 3979-3987.	3.1	19
15	Nanoparticles at Biomimetic Interfaces: Combined Experimental and Simulation Study on Charged Gold Nanoparticles/Lipid Bilayer Interfaces. Journal of Physical Chemistry Letters, 2019, 10, 129-137.	4.6	30
16	Regular Network of Misfit Dislocations at the BaZr _{0.8} Y _{0.2} O _{3â^'x} /NdGaO ₃ Interface and Its Role in Proton Conductivity. Physica Status Solidi (B): Basic Research, 2019, 256, 1800217.	1.5	6
17	Observation of Pore Growth and Self-Organization in Anodic Alumina by Time-Resolved X-ray Scattering. ACS Applied Nano Materials, 2018, 1, 1265-1271.	5.0	22
18	Poly-Amide Modified Copper Foam Electrodes for Enhanced Electrochemical Reduction of Carbon Dioxide. ACS Catalysis, 2018, 8, 4132-4142.	11.2	165

FRANCESCO CARLA

#	Article	IF	CITATIONS
19	In-plane molecular organization of hydrated single lipid bilayers: DPPC:cholesterol. Nanoscale, 2018, 10, 87-92.	5.6	16
20	Operando SXRD of E-ALD deposited sulphides ultra-thin films: Crystallite strain and size. Applied Surface Science, 2018, 432, 53-59.	6.1	5
21	Intermediate phase with orthorhombic symmetry displacement patterns in epitaxial PbZrO ₃ thin films at high temperatures. Ferroelectrics, 2018, 533, 26-34.	0.6	6
22	Self-organization of porous anodic alumina films studied <i>in situ</i> by grazing-incidence transmission small-angle X-ray scattering. RSC Advances, 2018, 8, 18980-18991.	3.6	17
23	In-situ synchrotron GIXRD study of passive film evolution on duplex stainless steel in corrosive environment. Corrosion Science, 2018, 141, 18-21.	6.6	32
24	Co film stretching induced by lattice mismatch and annealing: The role of Graphene. Applied Surface Science, 2018, 432, 22-26.	6.1	3
25	Structural Reorganization of Pt(111) Electrodes by Electrochemical Oxidation and Reduction. Journal of the American Chemical Society, 2017, 139, 4532-4539.	13.7	70
26	Integration of electrochemical and synchrotron-based X-ray techniques for in-situ investigation of aluminum anodization. Electrochimica Acta, 2017, 241, 299-308.	5.2	19
27	Operando SXRD study of the structure and growth process of Cu2S ultra-thin films. Scientific Reports, 2017, 7, 1615.	3.3	9
28	In situ studies of NO reduction by H ₂ over Pt using surface X-ray diffraction and transmission electron microscopy. Physical Chemistry Chemical Physics, 2017, 19, 8485-8495.	2.8	16
29	Controlling the growth of Bi(110) and Bi(111) films on an insulating substrate. Nanotechnology, 2017, 28, 155602.	2.6	20
30	Oxidation of CO on Pd(1Â0Â0): on the structural evolution of the PdO layer during the self sustained oscillation regime. Journal of Lithic Studies, 2017, 3, 89-94.	0.5	9
31	Initial stages of Pt(111) electrooxidation: dynamic and structural studies by surface X-ray diffraction. Electrochimica Acta, 2017, 224, 220-227.	5.2	71
32	Electrochemical Oxidation of Smooth and Nanoscale Rough Pt(111): An In Situ Surface X-ray Scattering Study. Journal of the Electrochemical Society, 2017, 164, H608-H614.	2.9	30
33	Pt oxide and oxygen reduction at Pt(111) studied by surface X-ray diffraction. Electrochemistry Communications, 2017, 84, 50-52.	4.7	18
34	Influence of C60 co-deposition on the growth kinetics of diindenoperylene–From rapid roughening to layer-by-layer growth in blended organic films. Journal of Chemical Physics, 2017, 146, 052807.	3.0	6
35	Multiple timescales in the photoswitching kinetics of crystalline thin films of azobenzene-trimers. Journal of Physics Condensed Matter, 2017, 29, 434001.	1.8	6
36	Electrochemical Formation of Germanene: pH 4.5. Journal of the Electrochemical Society, 2017, 164, D469-D477.	2.9	17

FRANCESCO CARLA

#	Article	IF	CITATIONS
37	Simultaneous scanning tunneling microscopy and synchrotron X-ray measurements in a gas environment. Ultramicroscopy, 2017, 182, 233-242.	1.9	8
38	Metal ion-exchange on the muscovite mica surface. Surface Science, 2017, 665, 56-61.	1.9	28
39	The structural evolution of graphene/Fe(110) systems upon annealing. Carbon, 2017, 111, 113-120.	10.3	9
40	Structure and Nanomechanics of Model Membranes by Atomic Force Microscopy and Spectroscopy: Insights into the Role of Cholesterol and Sphingolipids. Membranes, 2016, 6, 58.	3.0	35
41	Combined scanning probe microscopy and x-ray scattering instrument for in situ catalysis investigations. Review of Scientific Instruments, 2016, 87, 113705.	1.3	12
42	Synchrotron based operando surface Xâ€ray scattering study towards structure–activity relationships of model electrocatalysts. ChemistrySelect, 2016, 1, 1104-1108.	1.5	7
43	Epitaxial growth of gadolinium and lutetium-based aluminum perovskite thin films for X-ray micro-imaging applications. CrystEngComm, 2016, 18, 608-615.	2.6	31
44	The thickness of native oxides on aluminum alloys and single crystals. Applied Surface Science, 2015, 349, 826-832.	6.1	174
45	Custom AFM for X-ray beamlines: <i>in situ</i> biological investigations under physiological conditions. Journal of Synchrotron Radiation, 2015, 22, 1364-1371.	2.4	15
46	An in-situ X-ray diffraction study on the electrochemical formation of PtZn alloys on Pt(1 1 1) single crystal electrode. Applied Surface Science, 2015, 354, 443-449.	6.1	5
47	Surface alloying upon Co intercalation between graphene and Ir(111). Carbon, 2015, 94, 554-559.	10.3	27
48	Controlling the growth mode of <i>para</i> -sexiphenyl (6P) on ZnO by partial fluorination. Physical Chemistry Chemical Physics, 2014, 16, 26084-26093.	2.8	30
49	<i>In situ</i> anodization of aluminum surfaces studied by x-ray reflectivity and electrochemical impedance spectroscopy. Journal of Applied Physics, 2014, 116, .	2.5	17
50	Muscovite mica: Flatter than a pancake. Surface Science, 2014, 619, 19-24.	1.9	61
51	Synthesis and Technological Application of Electrodeposited Semiconductors by EC-ALD. ECS Transactions, 2014, 58, 35-41.	0.5	4
52	Dibenzo Crown Ether Layer Formation on Muscovite Mica. Langmuir, 2014, 30, 12570-12577.	3.5	9
53	Electrochemical Atomic Layer Deposition of CdS on Ag Single Crystals: Effects of Substrate Orientation on Film Structure. Journal of Physical Chemistry C, 2014, 118, 6132-6139.	3.1	20
54	Electrochemical characterization of core@shell CoFe2O4/Au composite. Journal of Nanoparticle Research, 2013, 15, 1.	1.9	14

FRANCESCO CARLA

#	Article	IF	CITATIONS
55	Physical Characterization of Thin Films of CuxZnySz for Photovoltaic Applications. ECS Transactions, 2013, 58, 59-65.	0.5	7
56	In-situ Monitoring of Electrochemical Oxidative Adsorption of Sulfur on Silver Single Crystals by Scanning Tunneling Microscopy. ECS Transactions, 2010, 25, 17-26.	0.5	2
57	Confined electrodeposition using a template-assisted procedure based on the selective desorption of a short chain thiol from a binary self-assembled monolayer formed on Ag(111). Electrochimica Acta, 2010, 55, 2550-2554.	5.2	6
58	Confined Electrodeposition of CdS in the Holes Left by the Selective Desorption of 3-Mercapto-1-propionic Acid from a Binary Self-Assembled Monolayer Formed with 1-Octanethiol. Langmuir, 2010, 26, 1802-1806.	3.5	5
59	In Situ Scanning Tunneling Microscopy Investigation of Sulfur Oxidative Underpotential Deposition on Ag(100) and Ag(110). Langmuir, 2010, 26, 17679-17685.	3.5	10
60	Combined electrochemical atomic layer epitaxy and microcontact printing techniques. Materials Science in Semiconductor Processing, 2009, 12, 21-24.	4.0	2
61	Nanopatterned Ag substrates for SERS spectroscopy. Physical Chemistry Chemical Physics, 2008, 10, 4555.	2.8	21
62	Phase Transitions and the Condition of Near-Interface Layer in PbZrO ₃ Epitaxial Films on SrRuO ₃ /SrTiO ₃ Substrate. Key Engineering Materials 0, 806, 93-99	0.4	0

Materials, 0, 806, 93-99.